



Dynamic light-responsive RhoA activity regulates mechanosensitive stem cell fate decision in 3D matrices

Jieung Baek^{a,b,c}, Sanjay Kumar^{a,b,*}, David V. Schaffer^{a,b,d,*}

^a Department of Chemical and Biomolecular Engineering, University of California, Berkeley, Berkeley, CA 94720, USA

^b Department of Bioengineering, University of California, Berkeley, CA 94720, USA

^c Division of Mechanical and Biomedical Engineering, Graduate Program in System Health Science and Engineering, Ewha Womans University, Seoul, 03760, Republic of Korea

^d Helen Wills Neuroscience Institute, Berkeley, CA 94720, USA

ARTICLE INFO

Keywords:

Neural stem cell (NSC)
Ras homolog family member A (RhoA) signaling
Mechanosensing
Early growth response (*Egr1*)
Optogenetics

ABSTRACT

The behavior of stem cells is regulated by mechanical cues in their niche that continuously vary due to extracellular matrix (ECM) remodeling, pulsated mechanical stress exerted by blood flow, and/or cell migration. However, it is still unclear how dynamics of mechanical cues influence stem cell lineage commitment, especially in a 3D microenvironment where mechanosensing differs from that in a 2D microenvironment. In the present study, we investigated how temporally varying mechanical signaling regulates expression of the early growth response 1 gene (*Egr1*), which we recently discovered to be a 3D matrix-specific mediator of mechanosensitive neural stem cell (NSC) lineage commitment. Specifically, we temporally controlled the activity of Ras homolog family member A (RhoA), which is known to have a central role in mechanotransduction, using our previously developed *Arabidopsis thaliana* cryptochrome-2-based optoactivation system. Interestingly, pulsed RhoA activation induced *Egr1* upregulation in stiff 3D gels only, whereas static light stimulation induced an increase in *Egr1* expression across a wide range of 3D gel stiffnesses. Actin assembly inhibition limited *Egr1* upregulation upon RhoA activation, implying that RhoA signaling requires an actin-involved process to upregulate *Egr1*. Consistently, static-light RhoA activation rather than pulsed-light activation restricted neurogenesis in soft gels. Our findings indicate that the dynamics of RhoA activation influence *Egr1*-mediated stem cell fate within 3D matrices in a matrix stiffness-dependent manner.

1. Introduction

It is known that the behavior of stem cells, including self-renewal and differentiation, is regulated by mechanical cues from their niches [1–4]. In particular, the native cellular niche subjects cells to spatiotemporally varying mechanical forces and force-dependent signals, since the niche is modified both acutely and chronically through in situ synthesis, localized degradation, and remodeling [4,5]. Furthermore, due to heart contraction, tissues including the brain experience oscillatory contraction [6,7]. In addition, cell movement and shape remodeling continuously exert dynamic mechanical forces on neighboring cells [8,9].

Mechanotransduction – the transduction of such mechanical cues into intracellular biochemical signals – involves several molecular signaling mechanisms ranging from stretch-activated ion channels to the activation of kinase cascades and GTPases [10–12]. One mechanism that

is centrally involved in many cellular responses to mechanical force is the activation of Ras homolog (Rho) family GTPases, particularly family member A (RhoA) [13–15]. In particular, RhoA signaling plays a key role in regulating the actin cytoskeleton, including actin polymerization and actomyosin contractility. By extension, RhoA functions as a key intermediary in transducing mechanical cues to regulate stem cell behavior such as fate commitment and differentiation. For example, our group previously found that signals transduced by RhoA and other small GTPases regulate mechanosensitive neural stem cell (NSC) lineage commitment on 2D substrates [16], with stiff 2D matrices inhibiting neurogenesis and promoting astrogenesis through activation of Rho GTPases.

While this and other studies [17] have established that RhoA activity regulates stem cell fate, the effect of spatiotemporal variation in Rho signaling on cell fate has not been broadly explored. Optogenetic control

* Corresponding authors at: Department of Chemical and Biomolecular Engineering, University of California, Berkeley, Berkeley, CA 94720, USA.

E-mail addresses: skumar@berkeley.edu (S. Kumar), schaffer@berkeley.edu (D.V. Schaffer).

<https://doi.org/10.1016/j.bioadv.2024.213836>

Received 18 January 2024; Received in revised form 5 March 2024; Accepted 19 March 2024

Available online 25 March 2024

2772-9508/© 2024 Published by Elsevier B.V.

has emerged as an important approach to investigate the complex nature of Rho-mediated contractility on mechanical forces [18] and to decipher mechanosensitive signaling pathways that regulate cell behavior [19]. For example, Ju et al. [20] observed that the amplitude of a single signal can induce distinct cell shapes through the rheostatic control of RhoA activity with a photoswitchable RhoA guanine nucleotide exchange factor (GEF). Furthermore, using a FRET sensor, we observed different RhoA activation dynamics on stiff vs. soft 2D gels, and using our previously developed *Arabidopsis thaliana* cryptochrome-2 (cry2)-based RhoA photoactivating system [21], we revealed that NSC lineage commitment is dependent on temporal variation of RhoA signaling on 2D substrates [22]. That is, increasing the pulse frequency of RhoA activation promoted astrogenesis while restricting neurogenesis.

However, most of these studies have been conducted based on 2D substrates, and 2D mechanosensory mechanisms do not necessarily translate into 3D systems that better emulate the natural tissue microenvironment [23–25]. In particular, we recently reported that early growth response 1 (*Egr1*) expression is upregulated in stiff 3D but not 2D matrices and mediates 3D matrix-specific mechanosensitive NSC lineage commitment [26]. *Egr1* knockdown rescued neurogenesis in 3D stiff gels, whereas it did not exhibit any significant effect in 2D gels. Furthermore, *Egr1* expression substantially dropped with osmotic manipulation of cell volume, supporting the idea that ECM confining stress, which exists in 3D and not in 2D, may contribute to 3D stiffness dependence of *Egr1* expression. In addition, it has also been reported that *Egr1* is rapidly upregulated by mechanical stimulation for Chinese hamster ovary (CHO) cells and is a downstream target of RhoA signaling during mechanotransduction in T cells [27,28]. These observations imply that *Egr1* is an important mediator of dynamic mechanical cues in the regulation of stem cell behavior in 3D matrices. However, the relationship between RhoA and *Egr1* has not been explored in 3D or in NSCs. In the present study, we encapsulated NSCs within hyaluronic acid (HA) hydrogels [29,30] at two different stiffness conditions (0.1 kPa: soft; 1.2 kPa: stiff) and found that RhoA activity fluctuated in a matrix stiffness-dependent manner with faster oscillation in stiffer 3D matrices. Furthermore, we observed that upon static blue light stimulation of cells expressing optogenetic RhoA, *Egr1* was upregulated within both soft and stiff matrices. However, intriguingly, only NSCs in stiff gels exhibited *Egr1* upregulation under pulsed-light activation, thereby demonstrating that dynamic RhoA activation regulates *Egr1* in a stiffness-dependent manner in a 3D microenvironment. Moreover, only static RhoA activation exhibited increased phalloidin intensity in 3D soft gels. Pharmacological inhibition of actin polymerization hampered *Egr1* upregulation upon both static and pulsed RhoA activation, indicating that RhoA-mediated *Egr1* upregulation involves actin assembly. Consistently, only static RhoA activation increased neurogenesis in 3D soft gels. In contrast, neither pulsed nor static RhoA activation significantly affected neurogenesis in stiff gels, potentially because the expression of *Egr1* was already sufficient to maximally restrict neurogenesis. Collectively, our findings uncover how the dynamics of RhoA signaling influence *Egr1*-mediated NSC lineage commitment in 3D matrices, which offers insights into how 3D-matrix stiffness regulates *Egr1* expression during mechanosensing.

2. Results

2.1. RhoA signaling regulates mechanosensitive NSC lineage commitment in 3D matrices

To investigate whether RhoA signaling influences NSC fate commitment in 3D matrices, we cultured cells within 3D gels in a differentiation medium that induces a mixture of neuronal and glial differentiation. Based on the stiffnesses of mammal brain tissues, which have been reported to range from 0.1 to 1.2 kPa, the stiffness in the same range was controlled by adjusting the molar ratio of azide (crosslinker) to HA monomer: ratio 0.02 for 0.1 kPa (soft) and 0.04 for 1.2 kPa (stiff)

[26]. Just after encapsulation of the cells with these gel formulations, we added a selective Rho-associated kinase (ROCK) inhibitor (Y27632) to the cells to block ROCK signaling, as well as dimethyl sulfoxide (DMSO) as a vehicle control for 3 h. There was no significant difference between cells in soft and stiff gels immediately after the encapsulation (0 h) (Fig. 1A). In contrast, after 3 h of encapsulation with DMSO treatment, we observed stiffness-dependent actin cytoskeletal assembly, with more intense cortical actin structures in stiff (1.2 kPa) than in soft (0.1 kPa) gels (Fig. 1B). This corresponds well with our previous study showing the same stiffness dependence of cytoskeletal assembly without any treatment [26]. However, the treatment with Y27632 qualitatively restricted actin formation in stiff gels. This result indicates that Rho/ROCK signaling regulates actin cytoskeletal assembly in 3D matrices. We next performed fluorescence immunostaining for neuronal (neuron-specific class III β -tubulin (Tuj1)) and astrocytic (glial fibrillary acidic protein (GFAP)) lineage markers after 7 days of encapsulation under vehicle- or Y27632-treated conditions (Fig. 1C and D). Consistent with our previous work [26], fate commitment was mechanosensitive in 3D matrices, with higher neurogenesis in soft gels. In contrast, Y27632 treatment reduced neurogenesis in soft gels to a similar level to that of stiff gels, and the opposite trend was observed for astrogenesis: the higher astrogenesis in stiff gels without Y27632 treatment was reciprocally diminished in gels with Y27632 treatment. These results imply that RhoA signaling plays an important role in mechanosensitive NSC lineage commitment in 3D matrices.

2.2. RhoA activity fluctuates in a mechanosensitive manner within a 3D microenvironment

We next examined RhoA activation dynamics in the soft and stiff 3D gels using NSCs expressing a fluorescence resonance energy transfer (FRET)-based RhoA biosensor (RhoA2G) [31]. The biosensor is a genetically encoded fusion of the RhoA-binding domain (RBD) of the effector rho-kinase with a donor fluorophore (mTFP1) and an acceptor fluorophore (Venus) for RhoA (Fig. 2A). The RBD binds guanosine triphosphate (GTP)-RhoA, the active form of RhoA [32], leading to a conformational change that brings Venus and mTFP1 in close proximity, thus increasing FRET intensity. After 3 h of 3D gel encapsulation in differentiation medium, we measured the spatiotemporal FRET intensity of RhoA2G-expressing NSCs (Fig. 2B). As has been previously described [22,31], the distribution of RhoA2G was mostly cytosolic and excluded from the nucleus. Moreover, interestingly, we observed that RhoA activity oscillated in NSCs within 3D matrices, and the periodicity depended on the stiffness of the 3D matrix (Fig. 2C and D). The mean of the RhoA oscillation period in soft gels (15.84 min) was more twice that in stiff gels (7.63 min). These results show that RhoA activation varies temporally with stiffness, thereby suggesting a role for RhoA dynamics in mechanosensitive NSC lineage commitment in 3D matrices.

2.3. Dynamic RhoA activation is more likely to upregulate *Egr1* in stiffer 3D gels

We next investigated whether the mechanosensitive behavior of NSCs in a 3D matrix is dependent on the temporal variation of RhoA activation. To temporally control RhoA activity, we utilized an optogenetic approach (Fig. 3A). We encapsulated NSCs expressing Cry2-RhoA (hereafter named 'optoRhoA' cells) [21] within 3D gels and controlled RhoA activation via blue light stimulation using a specialized LED illumination device (a light activation at variable amplitude (LAVA) device) that allows precise control of the light intensity and frequency [33]. Upon illumination, optoRhoA cells in both soft and stiff 3D gels showed an increase or enlargement in distinct fluorescent Cry2-mCherry-RhoA puncta within 6 min (Fig. 3B and C), consistent with our prior work demonstrating cluster formation and RhoA signal activation upon optoRhoA illumination [21,22].

We next focused on the expression of *Egr1* as an upstream regulator

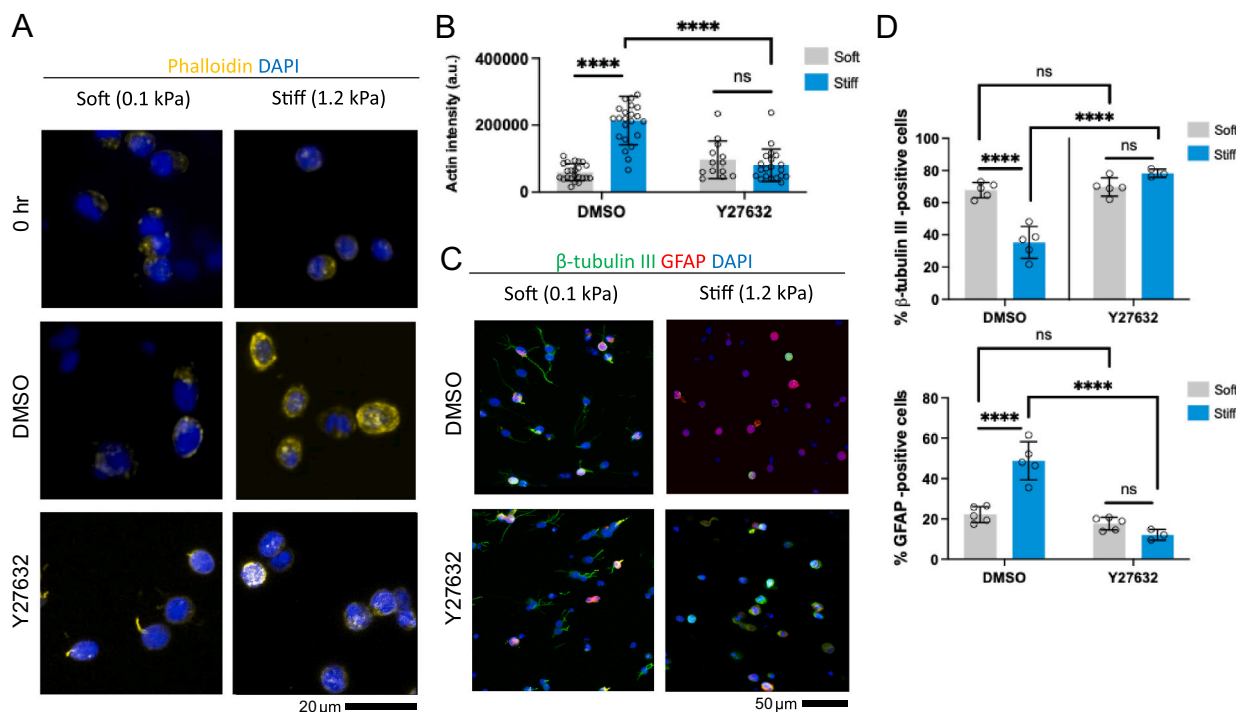


Fig. 1. Pharmacological inhibition of RhoA signaling perturbs mechanosensitive NSC lineage commitment in 3D matrices. (A) Representative phalloidin-stained NSCs in soft (0.1 kPa) and stiff (1.2 kPa) 3D matrices immediately following encapsulation (0 h) and after 3 h of encapsulation under DMSO or Y27632 (ROCKi, 10 μM)-treated condition (scale bar: 20 μm). (B) Quantification of peak cortex actin intensity line scan after background subtraction. (C) Immunofluorescence staining of NSCs differentiated in soft (0.1 kPa) and stiff (1.2 kPa) gels: neuronal lineage (β-tubulin III), green; astrocyte lineage (GFAP), red. The cells were treated with DMSO or Y27632 (ROCKi, 10 μM) for 48 h during differentiation (scale bar: 50 μm). (D) Quantification of the lineage marker-positive percentage of NSCs via immunofluorescence staining in (C). The results from n = 5 technical replicates with two biological replicates were subjected to one-way analysis of variance (ANOVA) followed by Tukey’s test. ****P < 0.001, ***P < 0.005, **P < 0.01, *P < 0.05. The bars in the graphs show the mean ± SD.

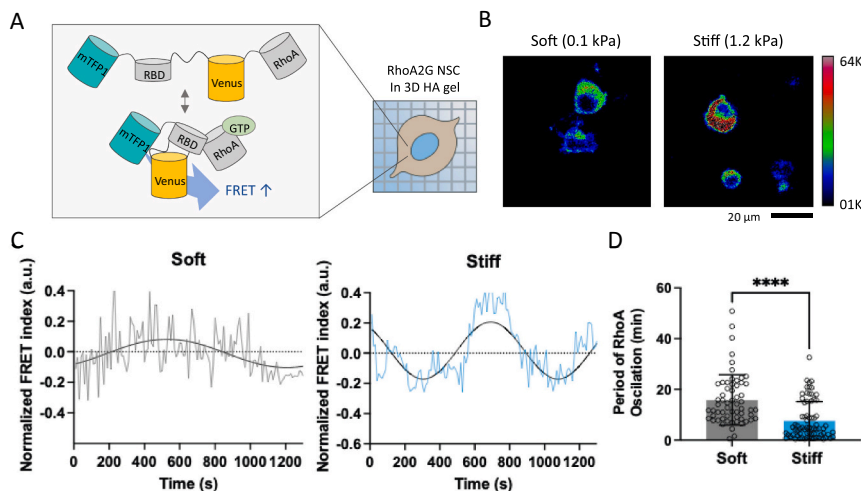


Fig. 2. NSCs exhibit mechanosensitive RhoA activity fluctuation in 3D matrices. (A) A schematic of the structure of the FRET biosensor (RhoA2G) to spatiotemporally visualize the RhoA activity of NSCs encapsulated within 3D gels. (B) FRET images of RhoA2G NSCs encapsulated within soft (0.1 kPa; left) and stiff (1.2 kPa; right) gels (scale bar: 20 μm; color bar represents FRET index). (C) Representative change of normalized FRET index over time. (D) Evaluation of the period of RhoA oscillation. The results from more than four regions of n > 9 cells per each set of conditions were subjected to Student t-test. ****P < 0.001, ***P < 0.005, **P < 0.01, *P < 0.05. The bars in the graphs show the mean ± SD.

of mechanosensitive NSC lineage commitment in response to RhoA activation. In a previous study, we discovered that *Egr1* is a 3D matrix-specific mediator of mechanosensitive NSC lineage commitment that restricts neurogenesis in stiffer gels [26]. Additionally, we found that the stiffness-dependent increase in *Egr1* expression is highly associated with

cortical actin assembly and pharmacologically induced RhoA activity. Furthermore, it has been reported that *Egr1* is rapidly upregulated in CHO cells in response to cyclic forces within 15 s [27]. With these observations in mind, we first investigated whether the intensity of blue light influences the mRNA expression level of *Egr1* in 3D matrices. To

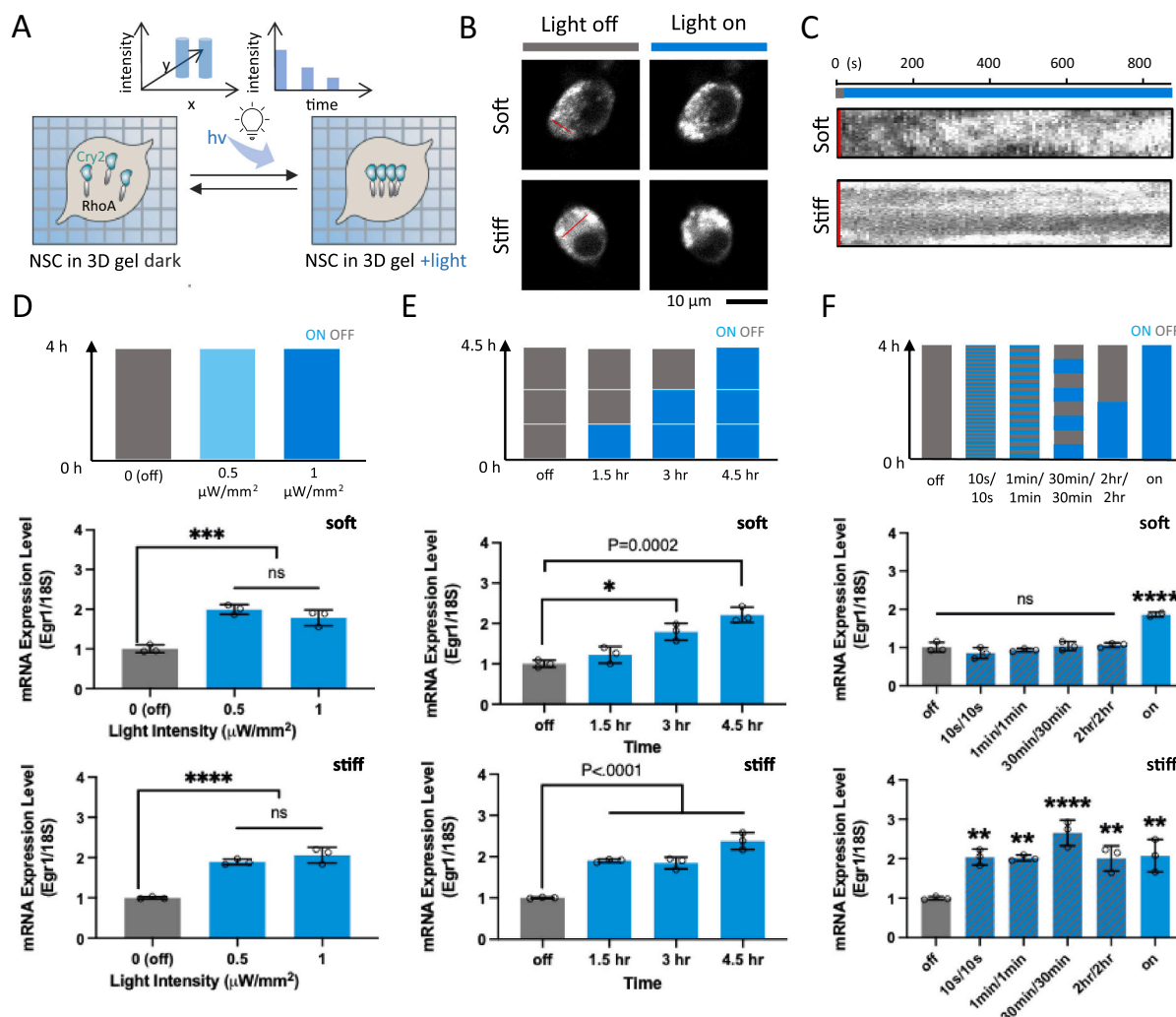


Fig. 3. Temporally varying RhoA activation upregulates *Egr1* in a matrix stiffness-dependent manner. (A) Schematic illustrations of the spatiotemporal optogenetic control of RhoA activity. Upon light ($h\nu$) activation, cry2-RhoA oligomerizes to activate RhoA signaling. (B) Illumination of NSCs expressing cry2-RhoA under static illumination (ON) or unilluminated (OFF) conditions. The cells were imaged after 3 h of encapsulation in soft (0.1 kPa) or stiff (1.2 kPa) 3D gels (scale bar: 10 μm). (C) Kymographs of cry2-RhoA fluorescence corresponding to the line in (B). (D) *Egr1* mRNA expression after 4 h of static light illumination under three different light intensity conditions (0.5, or 1 $\mu\text{W}/\text{mm}^2$) or no illumination. (E) *Egr1* mRNA expression levels under light stimulation over three different durations (1.5, 3, or 4.5 h) or no illumination. (F) *Egr1* mRNA expression levels under four different sets of light-pulsing conditions (10 s on/10 s off, 1 min on/1 min off, 30 min on/30 min off, or 2 h on/2 h off). Illumination = ON; no illumination = OFF. The total experimental time was kept at 4.5 h and the *Egr1* mRNA expression level was measured in cells in both soft and stiff 3D gels for each scenario. $n = 3$ technical replicates were analyzed using one-way ANOVA followed by a Tukey's test. **** $P < 0.001$, *** $P < 0.005$, ** $P < 0.01$, * $P < 0.05$. The bars in the graphs show the mean \pm SD.

this end, we illuminated cultures at three different intensities (0, 0.5, or 1 $\mu\text{W}/\text{mm}^2$) using LAVA devices directly after encapsulation in soft (0.1 kPa) or stiff (1.2 kPa) 3D gels (Fig. 3D). After 4 h of static illumination, cells were harvested to measure the *Egr1* expression level via qPCR. Blue light illumination at an intensity of 0.5 or 1 $\mu\text{W}/\text{mm}^2$ increased *Egr1* expression in cells embedded in both soft and stiff 3D gels compared to no illumination. Both 0.5 $\mu\text{W}/\text{mm}^2$ and 1 $\mu\text{W}/\text{mm}^2$ for 4 h led to similar *Egr1* expression, potentially because the lower dose already saturated the *Egr1* expression level, leading to no further statistically significant increase in the *Egr1* expression under elevation to 1 $\mu\text{W}/\text{mm}^2$. The difference in the overall light dosages for 0.5 $\mu\text{W}/\text{mm}^2$ and 1 $\mu\text{W}/\text{mm}^2$ over 4 h was not sufficient to induce a difference in *Egr1* expression. This may be because the total dosage at 0.5 $\mu\text{W}/\text{mm}^2$ is already sufficient to induce the maximum possible increase in *Egr1* expression, leading to no further statistically significant increase in the *Egr1* expression under the 1 $\mu\text{W}/\text{mm}^2$ intensity condition. Given these results, we next sought to see whether light duration at 1 $\mu\text{W}/\text{mm}^2$ influences the *Egr1* expression

level in 3D matrices. To this end, we illuminated cells for three different durations (1.5, 3, or 4.5 h) while maintaining a total encapsulation time of 4.5 h for each experiment (Fig. 3E). Intriguingly, only 3 and 4 h of illumination induced statistically significant increases in *Egr1* expression within soft 3D gels, whereas within stiff 3D gels, *Egr1* was upregulated under all of the light durations, including 1.5 h.

Given that the Cry2 clustering-based optogenetic system enables the translocation of RhoA to membranes or vesicles within seconds of light activation [21], we also illuminated optoRhoA cells under three different sets of light-pulsing conditions (10 s on/10 s off, 1 min on/1 min off, 30 min on/30 min off, or 2 h on/2 h off) or static illumination (Fig. 3F). Light intensity (1 $\mu\text{W}/\text{mm}^2$) and total illumination time (4 h) – and thus overall light dosage – were kept the same under all the light-pulsing conditions. Notably, cells in soft gels exhibited *Egr1* upregulation only under static illumination and not under any of the light-pulsing scenarios. In contrast, increased *Egr1* expression by cells within stiff gels was observed under all the light-pulsing and static illumination

scenarios. Even though the total dose of light in each light-pulsing condition was half that under static illumination, the degree of *Egr1* upregulation in cells within stiff gels was the same. This could be related to the previous finding that there is no statistical difference in *Egr1* expression under light intensities of 0.5 and 1 $\mu\text{W}/\text{mm}^2$ for 4 h (Fig. 3D).

2.4. Activated RhoA signaling upregulates *Egr1* through a cytoskeletal actin-involved process

In prior work [26], we observed that stiffness-dependent *Egr1* expression in 3D was highly associated with actin assembly. Cortical actin formed more intensely in stiffer gels, and pharmacological inhibition of this assembly blocked *Egr1* upregulation, showing increased neurogenesis. We thus next investigated whether the RhoA-mediated *Egr1* upregulation in 3D matrices is associated with altered cytoskeletal assembly. We first observed actin formation by imaging phalloidin-stained optoRhoA NSCs in soft and stiff 3D gels under vehicle- and actin assembly inhibitor cytochalasin D (cyt D)-treated conditions (Fig. 4A). Immediately after encapsulation, we stimulated NSCs with blue light to control RhoA activity with pulsed 10 s on/10 s off or static illumination, the duration of which is closest to the reported shortest duration (15 s) of mechanical stimulation for *Egr1* upregulation [27]. We maintained constant intensity (1 $\mu\text{W}/\text{mm}^2$) for 4 h of encapsulation, after which the cells were fixed for imaging. Consistent with our previous findings [26], cells in stiff gels with vehicle without light stimulation showed higher actin intensity than those in soft gels under the same conditions. Furthermore, activation of RhoA through static illumination caused more intense actin assembly in cells in both soft and stiff gels compared to no illumination. On the other hand, surprisingly, pulsed illumination (10 s on/10 s off) did not significantly affect actin cytoskeletal formation in cells in both soft and stiff gels compared to without illumination. Consequently, cells still maintained stiffness-dependent cytoskeletal

formation under the pulsed illumination. These results indicate that only static light stimulation promotes actin cytoskeletal assembly. Meanwhile, treatment with cyt D restricted actin assembly, leading less intensely formed cytoskeletal structures compared to corresponding vehicle-treated cells in all conditions. Based on these outcomes, we next examined whether *Egr1* expression was perturbed after the inhibition of actin assembly (Fig. 4B). Although static illumination enabled the upregulation of *Egr1* in cells in both the soft and stiff 3D gels, only those in stiff gels exhibited increased *Egr1* expression under pulsed-light (10 s on/10 s off) illumination, corresponding well with what we previously observed (Fig. 3F). Notably, however, impairing actin assembly prevented *Egr1* upregulation with either static or pulsed (10 s on/10 s off) illumination. Taken together, our findings indicate that RhoA-mediated *Egr1* upregulation under both pulsed and static light stimulation within stiff gels is highly associated with actin cytoskeletal assembly. This is consistent with our previous finding that *Egr1* expression only increases in stiff gels under pulsed-light stimulation (Fig. 3F), indicating that some level of matrix-induced actin assembly is required for pulsed RhoA activation to increase *Egr1* expression.

2.5. RhoA activation decreases neurogenesis in cells only in soft gels

We previously found that higher *Egr1* expression in stiff gels restricts neuronal lineage commitment by suppressing β -catenin signaling [26]. Given the stiffness-dependent role of dynamic RhoA activation in *Egr1* upregulation, we next investigated whether dynamic RhoA activation influenced NSC lineage commitment. OptoRhoA NSCs in soft (0.1 kPa) and stiff (1.2 kPa) 3D gels were incubated for 7 days in differentiation media (Fig. 5A), and cells were stimulated with blue light (1 $\mu\text{W}/\text{mm}^2$) under pulsed (10 s on/10 s off) or static conditions, or in the dark, for 18 h. Static illumination under conditions we previously found induced *Egr1* upregulation (Fig. 3D), decreased neurogenesis at 7 days in soft gels only, while astrogenesis increased (Fig. 5B). This result corresponds well with our previous finding that *Egr1* overexpression decreases neurogenesis in cells in 3D soft gels only [26]. No significant reduction in neurogenesis was observed in stiff gels under both static and pulsed-light illumination despite *Egr1* upregulation under these conditions. This outcome implies that although *Egr1* was further upregulated in stiff gels through light stimulation (Fig. 3D–F), the levels could have already been sufficient to maximally suppress neurogenesis. In contrast, the decrease in neurogenesis of cells in soft gels upon pulsed illumination was not as pronounced as that upon static illumination. This is consistent with *Egr1* upregulation only occurring in cells within soft 3D gels upon static illumination (Fig. 3F). In sum, our results indicate that NSC lineage commitment in soft 3D gels is biased toward astrogenesis through static-but not pulsed-illumination mediated RhoA activation (Fig. 5C).

3. Discussion

Investigating how stem cells respond to not only static but also temporally varying mechanical signals may advance our understanding of stem cell fate regulation in natural tissue environments. In this study, we observed dynamic, stiffness-dependent RhoA activation in 3D matrices with a FRET-based RhoA2G biosensor, i.e. RhoA activity oscillated with shorter periods in stiff gels than in soft gels. Given this finding, we investigated whether and how dynamic RhoA activation regulated *Egr1*-mediated NSC fate commitment in a 3D microenvironment through Cry2 clustering-based optogenetic temporal control. Temporally varied illumination of optoRhoA cells within 3D matrices revealed that dynamic RhoA activation regulated *Egr1* expression in a matrix stiffness-dependent manner. Pulsed-light stimulation increased *Egr1* expression in stiff gels but not in soft gels. In addition, inhibition of actin assembly restricted this *Egr1* upregulation under both static and dynamic illumination conditions, thereby indicating that RhoA signaling-mediated *Egr1* upregulation involves an actin-mediated process. Consistent with the inhibitory role of *Egr1* on neurogenesis in 3D

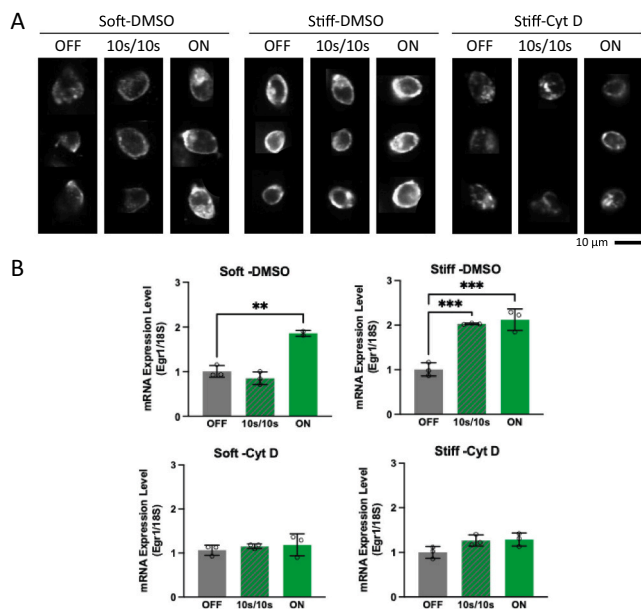


Fig. 4. Activated RhoA signaling upregulates *Egr1* through an actin-involved process. (A) Representative microscopic images of phalloidin-stained optoRhoA NSCs in a soft gel (0.1 kPa) after the treatment of DMSO and in a stiff gel (1.2 kPa) after treatment with DMSO or cytochalasin D (cyt D; 1 μM) for 4 h. The light was applied statically (ON), pulsed (10 s on/10 s off), or else not applied (OFF) for 4 h immediately after encapsulation. Scale bar: 10 μm . (B) *Egr1* mRNA expression levels in soft and stiff gels after treatment of DMSO or cytochalasin Dv (1 μM) for 4 h. $n = 3$ technical replicates were analyzed via one-way ANOVA followed by a Tukey's test. **** $P < 0.001$, *** $P < 0.005$, ** $P < 0.01$, * $P < 0.05$. The bars in the graphs show the mean \pm SD.

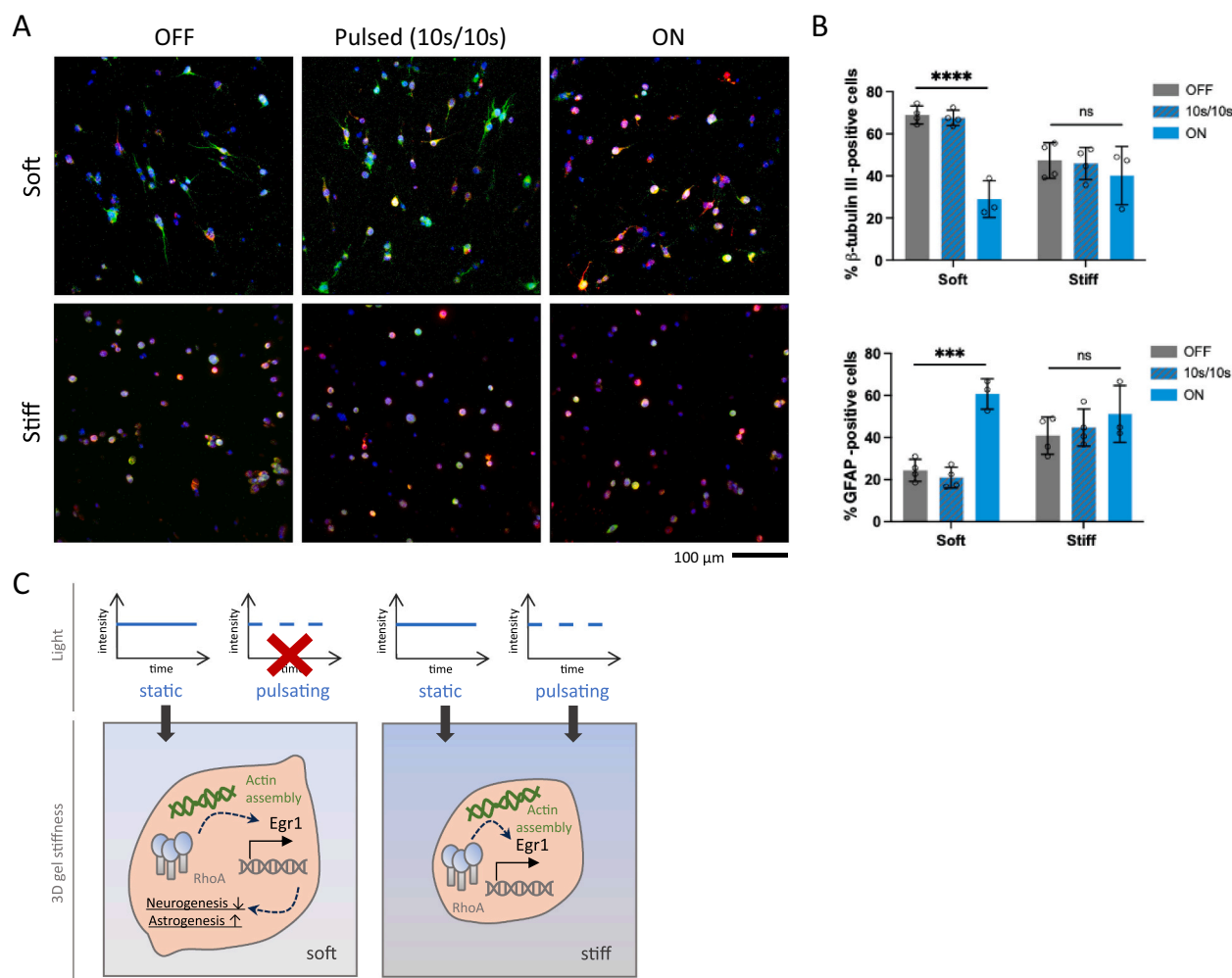


Fig. 5. Activating RhoA signaling decreased neurogenesis in soft gels only. (A) Immunofluorescence staining of optoRhoA NSCs in soft (0.1 kPa) and stiff (1.2 kPa) 3D gels incubated in media that support both neuronal and astrocytic differentiation for 7 days. Three different light stimulation conditions were applied for 18 h directly after encapsulation: unilluminated (OFF), pulsed-light (10 s on/10 s off), or statically illuminated (ON). Neuronal lineage (β -tubulin III), green; astrocyte lineage (GFAP), red (scale bar: 100 μ m). (B) Quantification of β -tubulin III- and GFAP-positive cells differentiated in the soft and stiff 3D gels under the three different light stimulation conditions mentioned in (A). (C) An illustration showing the suggested mechanism of RhoA activation-mediated *Egr1* upregulation and modulation NSC fate commitment in 3D gels. $n = 3$ or 4 technical replicates with two biological replicates were analyzed via one-way ANOVA followed by Tukey’s tests. **** $P < 0.001$, *** $P < 0.005$, ** $P < 0.01$, * $P < 0.05$. The bars in the graphs show the mean \pm SD.

matrices, static light stimulation decreased the neurogenesis of cells in soft gels, but pulsed-light activation did not. In contrast, despite the increased *Egr1* expression upon static or pulsed-light stimulation of cells in stiff gels, the cells exhibited neither promoted astrogenesis nor further suppressed neurogenesis. This corresponds well with our previous finding that overexpression of *Egr1* alters the NSC fate bias in soft gels but not in stiff gels [26].

RhoA activation under all the pulsed-light conditions with durations of 10 s or longer increased *Egr1* expression in stiff gels. However, notably, this occurred only in a stiff matrix, implying that the latter provides more favorable conditions for *Egr1* upregulation, potentially due to stiffness-dependent actin cytoskeletal formation in 3D matrices. Disruption of actin assembly limited *Egr1* upregulation under both static- and pulsed-light RhoA activation, indicating that *Egr1* upregulation triggered by RhoA activation requires actin assembly. This supports our previous finding of lower *Egr1* expression after the inhibition of actin assembly [26], which could be because endogenous RhoA activation cannot upregulate *Egr1* when actin polymerization is restricted. Furthermore, although it is known that RhoA activation plays an important role in actin assembly, only static-light stimulation of RhoA activation promoted actin formation in cells in 3D gels whereas pulsed

illumination was insufficient to stimulate it. Considering this outcome, dynamic stimulation may be more likely to upregulate *Egr1* in cells in stiff gels than in soft gels because the former tend to have more highly assembled actin networks that prime the cell for RhoA activation-mediated *Egr1* upregulation.

Different cellular responses to static vs. dynamic mechanical signals have been reported previously. Our previous work has shown that the frequency of RhoA activation regulates NSC fate commitment in 2D substrates by influencing the persistence of SMAD1/5, a transcription factor that promotes astrocytic differentiation [22]. While *Egr1* expression was not clearly dependent on the slightly different frequencies of RhoA activation in the present study, the dynamic RhoA activation may modulate the *Egr1* expression depending on the stiffness of 3D matrices. Since several studies have shown that *Egr1* is an immediate early gene (IEG) rapidly upregulated by external stimuli [27], it could be an important target for understanding how cells modulate gene regulation in response to dynamic mechanical cues. Sun et al. reported that the transcription of *Egr1* in CHO cells is upregulated by cyclic forces at low frequencies on 2D substrates by unraveling chromatin and then inducing an enrichment of RNA Pol II to the transcription region [27].

However, little is known about the causal link between *Egr1*

expression and dynamic mechanical cues within a 3D microenvironment, which better mimics a natural tissue environment. Considering this, our findings may provide novel insight into how cells process dynamic mechanical signals in a 3D microenvironment, which cannot be revealed via 2D substrate-based studies.

4. Conclusions

In summary, we have revealed a 3D stiffness-dependent relationship between dynamic RhoA activation as a function of optogenetic RhoA stimulation and mechanosensitive stem cell lineage commitment mediated by *Egr1*. In the future, it would be fruitful to reveal how RhoA activation, chromatin perturbation, and *Egr1* transcription are linked. Furthermore, elucidating how rapid cytoskeletal formation and *Egr1* expression on a timescale of few minutes under temporally varied mechanical cues are integrated into long term changes in cell fate.

5. Online methods

5.1. NSC culture

Adult rat hippocampal NSCs derived from female Fischer 344 rats (Charles River) were cultured in Dulbecco's modified Eagle's medium/nutrient mixture F-12 (DMEM-F-12, Gibco) with N-2 supplementation (Life Technologies) and fibroblast growth factor (FGF)-basic (20 ng/ml; Peprotech). During culture, cells adhered to the tissue-culture polystyrene plates sequentially coated with poly-ornithine (10 µg/ml, Sigma-Aldrich) and laminin (5 µg/ml, Invitrogen), and the medium was replenished every 2 days. Cells were then treated with N-2 supplemented DMEM-F-12 for cell culturing our established mixed differentiation medium containing retinoic acid (1 µM for the neuronal lineage) and fetal bovine serum (1 % for the astrocytic lineage) [16]. The differentiation medium was also replenished every 2 days. After 7 days of differentiation, the cells were fixed for immunofluorescence imaging.

5.2. NSC encapsulation

HA (average molecular weight 66–99 kDa, Lifecore Biomedical) was functionalized with dibenzocyclooctyne (DBCO) groups via *N*-hydroxysuccinimide (NHS)/*N*-(3-dimethylaminopropyl)-*N*-ethylcarbodiimide (EDC) activation as previously described [27]. Subsequently, DBCO-functionalized HA (HA-DBCO) was crosslinked to form hydrogels through strain-promoted azide-alkyne cycloaddition (SPAAC) between azide and DBCO functional groups by using polyethylene glycol (PEG)-bis (azide) (Sigma) as a crosslinker. Furthermore, an RGD sequence-containing peptide with azide functionality (K(N₃)GS-GRGDSPG, 1 mM, Genscript) was used to induce integrin binding of the cells. Encapsulation of the NSCs was carried out by incubating a mixture of HA-DBCO, PEG-bis (azide), the RGD peptide, and the cells for 10 min at 37 °C. Finally, the cells were differentiated immediately after encapsulation to start each experiment.

5.3. RNA isolation and qPCR

RNA extraction and quantitative polymerase chain reaction (qPCR) were performed to analyze the NSCs obtained from HA-DBCO gels. The gels were incubated in DMEM/F-12 containing hyaluronidase (750–3000 U/ml, Sigma Aldrich) for 30 min at 37 °C to extract the NSCs. The resulting suspensions were centrifuged at 200 ×g for 2 min to pellet cells, which were then washed with PBS. Total RNA was extracted from the cell pellets using the RNeasy Plus Micro Kit with gDNA eliminator columns (Qiagen) following the manufacturer's protocol. After measuring the total RNA concentration, 600 ng of RNA was converted to cDNA using the iScript cDNA synthesis kit (Bio-Rad). The obtained cDNA was utilized for SYBR Green (Bimake) qPCR with a final concentration of 5 µM for both forward and reverse primers (*Egr1*-F:

GTATGCTTGCCCTGTTGAGTCC; *Egr1*-R: CATGCAGATTCGA-CACTGGAAG; 18S-F: GTAACCCGTTGAACCCCATTC; 18S-R: CCATC-CAATCGGTAGTAGCGA), as shown in our previous study [26]. The qPCR was conducted for 34 cycles in a CFX connect real-time PCR system (Bio-Rad). RNA level analysis was performed using the ddCt method, and each gene expression was internally normalized by the expression level of the housekeeping gene S18, run on the same qPCR batch.

5.4. Immunocytochemistry

NSCs in 3D gels were fixed with 4 % paraformaldehyde (Sigma) for 15 min at room temperature. After washing three times with phosphate-buffered saline (PBS), the NSCs within each gel were fixed by incubating with a 4 % paraformaldehyde solution (Sigma) for 15 min at room temperature (RT). Fixed cells were incubated with Triton X-100 (0.3 % w/v, Sigma) and bovine serum albumin (BSA; 1 % w/v) in D-PBS (Dulbecco's PBS) solution for 30 min at RT, and then washed with D-PBS. Samples were then incubated at 4 °C for 48 h with the following primary antibodies: mouse anti-N-cadherin (1:500, C3865, Sigma), mouse anti-Tubulin β 3 (TUBB3) (1:1000, 801201, BioLegend), rabbit anti-GFAP (1:1000, ab7260, Abcam), mouse anti-vinculin (1:200, ab18058, Abcam), and mouse anti-active-β-catenin (1:200, 05-665, Millipore). After washing with D-PBS, the resulting samples were stained with goat anti-mouse IgG (H + L) secondary antibody, Alexa fluor 488 (1:250, cat. no. A11001; Invitrogen) or goat anti-rabbit IgG (H + L) secondary antibody, Alexa fluor 633 (1:250, cat. no. A21070; Invitrogen) for 40 min at RT, and then with 4',6-diamidino-2-phenylindole (DAPI, Sigma) for 10 min to counterstain cell nuclei. Cytoskeletons were stained with Rhodamine Phalloidin (1:40, cat. no. R415; Invitrogen). Fluorescent images were visualized via z-stacking with a confocal laser-scanning microscope (LSM 880, Carl Zeiss).

5.5. RhoA FRET biosensor characterization

To assess the temporal variation of Rho GTPase activation in NSCs, the latter were transduced with a viral vector for expressing a RhoA FRET sensor (RhoA2G) [31]. The transduced RhoA2G cells were encapsulated in soft (0.1 kPa) or stiff (1.2 kPa) 3D gels for 3 h and measured by using a live cell chamber in the confocal microscope. The donor was excited at 453 nm and emission from 520 to 580 nm was recorded every 10 s. The spatiotemporal FRET intensity was calculated using the FRET analyzer plugin in ImageJ. The periodicity of RhoA activation oscillation was obtained by using sine-fitting in ORIGIN.

5.6. Optogenetic stimulation

OptoRhoA NSCs were encapsulated in soft (0.1 kPa) or stiff (1.2 kPa) 3D gels in 24-well plates (0030741021, Eppendorf, black-walled with a 170 µm coverglass bottom) and loaded onto LAVA illumination devices [33] kept under standard tissue-culture conditions (37 °C). Optogenetic stimulation was performed with blue light at 470 nm for the desired temporal variations (static or pulsed) for 4–4.5 h in differentiation medium.

5.7. Statistical analysis

Data are expressed as mean ± SD. Statistical comparisons were conducted using independent example *t*-tests or one-way analysis of variance (ANOVA) with Tukey's tests used to make pairwise comparisons between multiple groups. Statistical significance was set to $p < 0.05$.

CRedit authorship contribution statement

Jieung Baek: Writing – review & editing, Writing – original draft,

Visualization, Validation, Methodology, Investigation, Formal analysis, Data curation, Conceptualization. **Sanjay Kumar:** Writing – review & editing, Writing – original draft, Validation, Supervision, Project administration, Funding acquisition, Conceptualization. **David V. Schaffer:** Writing – review & editing, Writing – original draft, Validation, Supervision, Project administration, Funding acquisition, Conceptualization.

Declaration of competing interest

The authors declare that they have no known competing financial interests or personal relationships that could have appeared to influence the work reported in this paper.

Data availability

No data was used for the research described in the article.

Acknowledgments

This work was supported by National Institutes of Health grant R01NS074831 (S.K., D.V.S.) and the National Research Foundation of Korea (NRF) grant funded by the Korean government (MSIT) (No. RS-2023-00213047).

References

- W.-T. Hsieh, Y.-S. Liu, Y.-H. Lee, M.G. Rimando, K.-H. Lin, O.K. Lee, Matrix dimensionality and stiffness cooperatively regulate osteogenesis of mesenchymal stromal cells, *Acta Biomater.* 32 (2016) 210–222.
- C. Kothapalli, G. Mahajan, K. Farrell, Substrate stiffness induced mechanotransduction regulates temporal evolution of human fetal neural progenitor cell phenotype, differentiation, and biomechanics, *Biomater. Sci.* 8 (19) (2020) 5452–5464.
- N.D. Leipzig, M.S. Shoichet, The effect of substrate stiffness on adult neural stem cell behavior, *Biomaterials* 30 (36) (2009) 6867–6878.
- W.L. Murphy, T.C. McDevitt, A.J. Engler, Materials as stem cell regulators, *Nat. Mater.* 13 (6) (2014) 547.
- D. Mohammed, M. Versaavel, C. Bruyère, L. Alaimo, M. Luciano, E. Vercruyse, A. Procès, S. Gabriele, Innovative tools for mechanobiology: unraveling outside-in and inside-out mechanotransduction, *Front. Bioeng. Biotechnol.* 7 (2019).
- A.L. Adams, H.J. Kuijf, M.A. Viergever, P.R. Luijten, J.J.M. Zwanenburg, Quantifying cardiac-induced brain tissue expansion using DENSE, *NMR Biomed.* 32 (2) (2019) e4050.
- T. Meyer, B. Kreft, J. Bergs, E. Antes, M.S. Anders, B. Wellge, J. Braun, M. Doyley, H. Tzschätzsch, I. Sack, Stiffness pulsation of the human brain detected by non-invasive time-harmonic elastography, *Front. Bioeng. Biotechnol.* 11 (2023).
- T. Luque, M.S. Kang, D.V. Schaffer, S. Kumar, Microelastic mapping of the rat dentate gyrus, *R. Soc. Open Sci.* 3 (4) (2016) 150702.
- D. Pinheiro, Y. Bellaïche, Mechanical force-driven adherens junction remodeling and epithelial dynamics, *Dev. Cell* 47 (1) (2018) 3–19.
- K.A. Jansen, P. Atherton, C. Ballestrem, Mechanotransduction at the cell-matrix interface, *Semin. Cell Dev. Biol.* 71 (2017).
- C. Argentati, F. Morena, I. Tortorella, M. Bazzucchi, S. Porcellati, C. Emiliani, S. Martino, Insight into mechanobiology: how stem cells feel mechanical forces and orchestrate biological functions, *Int. J. Mol. Sci.* 20 (21) (2019) 5337.
- J. Baek, W.-B. Jung, Y. Cho, E. Lee, G.-T. Yun, S.-Y. Cho, H.-T. Jung, S. Im, Facile fabrication of high-definition hierarchical wrinkle structures for investigating the geometry-sensitive fate commitment of human neural stem cells, *ACS Appl. Mater. Interfaces* 11 (19) (2019) 17247–17255.
- K. Burridge, E. Monaghan-Benson, D.M. Graham, Mechanotransduction: from the cell surface to the nucleus via RhoA, *Philos. Trans. R. Soc. B Biol. Sci.* 374 (1779) (2019) 20180229.
- A. Hall, Rho GTPases and the actin cytoskeleton, *Science* 279 (5350) (1998) 509–514.
- J. Baek, S.-Y. Cho, H. Kang, H. Ahn, W.-B. Jung, Y. Cho, E. Lee, S.-W. Cho, H.-T. Jung, S. Im, Distinct mechanosensing of human neural stem cells on extremely limited anisotropic cellular contact, *ACS Appl. Mater. Interfaces* 10 (40) (2018) 33891–33900.
- A.J. Keung, E.M.D. Juan-Pardo, D.V. Schaffer, S. Kumar, Rho GTPases mediate the mechanosensitive lineage commitment of neural stem cells, *Stem Cells* 29 (11) (2011) 1886–1897.
- R. McBeath, D.M. Pirone, C.M. Nelson, K. Bhadriraju, C.S. Chen, Cell shape, cytoskeletal tension, and RhoA regulate stem cell lineage commitment, *Dev. Cell* 6 (4) (2004) 483–495.
- V. Emiliani, E. Entcheva, R. Hedrich, P. Hegemann, K.R. Konrad, C. Lüscher, M. Mahn, Z.-H. Pan, R.R. Sims, J. Vierock, O. Yizhar, Optogenetics for light control of biological systems, *Nat. Rev. Method. Prim.* 2 (1) (2022) 55.
- E.E. Berlew, I.A. Kuznetsov, K. Yamada, L.J. Bugaj, J.D. Boerckel, B.Y. Chow, Single-component optogenetic tools for inducible RhoA GTPase signaling, *Adv. Biol.* 5 (9) (2021) 2100810.
- J. Ju, H. Lee, L. Ning, H. Ryu, X.X. Zhou, H. Chun, Y. Lee, A.I. Lee-Richerson, C. Jeong, M.Z. Lin, J. Seong, Optical regulation of endogenous RhoA reveals selection of cellular responses by signal amplitude, *Cell Rep.* 40 (2) (2022) 111080.
- L.J. Bugaj, A.T. Choksi, C.K. Mesuda, R.S. Kane, D.V. Schaffer, Optogenetic protein clustering and signaling activation in mammalian cells, *Nat. Methods* 10 (3) (2013) 249–252.
- R.G. Sampayo, M. Sakamoto, M. Wang, S. Kumar, D.V. Schaffer, Mechanosensitive stem cell fate choice is instructed by dynamic fluctuations in activation of Rho GTPases, *Proc. Natl. Acad. Sci.* 120 (22) (2023).
- A. Saraswathibhatla, D. Indana, O. Chaudhuri, Cell–extracellular matrix mechanotransduction in 3D, *Nat. Rev. Mol. Cell Biol.* 24 (7) (2023) 495–516.
- A.D. Doyle, K.M. Yamada, Mechanosensing via cell-matrix adhesions in 3D microenvironments, *Exp. Cell Res.* 343 (1) (2015) 60–66.
- B.M. Baker, C.S. Chen, Deconstructing the third dimension — how 3D culture microenvironments alter cellular cues, *J. Cell Sci.* 125 (13) (2012) 3015–3024.
- J. Baek, P.A. Lopez, S. Lee, T.-S. Kim, S. Kumar, D.V. Schaffer, Egr1 is a 3D matrix-specific mediator of mechanosensitive stem cell lineage commitment, *Sci. Adv.* 8 (15) (2022) eabm4646.
- J. Sun, J. Chen, E. Mohagheghian, N. Wang, Force-induced gene up-regulation does not follow the weak power law but depends on H3K9 demethylation, *Sci. Adv.* 6 (14) (2020) eaay9095.
- M. Mullin, K. Lightfoot, R. Clarke, M. Miller, R. Lahesmaa, D. Cantrell, The RhoA transcriptional program in pre-T cells, *FEBS Lett.* 581 (22) (2007) 4309–4317.
- M.M. Adil, T. Vazin, B. Ananthanarayanan, G. Rodrigues, A.T. Rao, R.U. Kulkarni, E.W. Miller, S. Kumar, D.V. Schaffer, Engineered hydrogels increase the post-transplantation survival of encapsulated hESC-derived midbrain dopaminergic neurons, *Biomaterials* 136 (2017) 1–11.
- J. Baek, S. Kumar, D.V. Schaffer, S.G. Im, N-cadherin adhesive ligation regulates mechanosensitive neural stem cell lineage commitment in 3D matrices, *Biomater. Sci.* 10 (23) (2022) 6768–6777.
- R.D. Fritz, M. Letzelter, A. Reimann, K. Martin, L. Fusco, L. Ritsma, B. Ponsoen, E. Fluri, S. Schulte-Merker, J.V. Rheenen, O. Pertz, A versatile toolkit to produce sensitive FRET biosensors to visualize signaling in time and space, *Sci. Signal.* 6 (285) (2013) rs12.
- E.-K. Choi, J.-G. Kim, H.-J. Kim, J.-Y. Cho, H. Jeong, Y. Park, R. Islam, C.K. Cap, J.-B. Park, Regulation of RhoA GTPase and novel target proteins for ROCK, *Small GTPases* 11 (2) (2020) 95–102.
- N.A. Repina, T. McClave, H.J. Johnson, X. Bao, R.S. Kane, D.V. Schaffer, Engineered illumination devices for optogenetic control of cellular signaling dynamics, *Cell Rep.* 31 (10) (2020) 107737.